# Investigation into the Phosphorescence of a Series of Regioisomeric Iridium(III) Complexes

Hugo A. Bronstein,[†] Chris E. Finlayson,[‡] Kiril R. Kirov,[‡] Richard H. Friend,[‡] and Charlotte K. Williams*,[†]

*Department of Chemistry, Imperial College London, London, SW7 2AZ, U.K., and Optoelectronics Group, Cavendish Laboratory, Cambridge University, JJ Thompson Avenue, Cambridge CB3 0HE, U.K.*

*Received January 7, 2008*

A series of heteroleptic cyclometalated Ir(III) complexes with the general structure [Ir(piq-X)$_2$(acac)] (where piq = 1-phenylisoquinolato, X = bromine, 9,9-dioctyl-2-fluorenyl, poly(9,9-dioctyl-2,7-fluorene), acac = acetyl acetonate) have been prepared. The complexes are regioisomers where the X substituents occupy positions 2, 3, or 4 on the phenyl ring. The isomers all show red phosphorescence but have varying wavelengths and quantum yields. The nature and site of substitution influence the energy and localization of the frontier molecular orbitals, and this is investigated using electrochemistry, absorption and emission spectroscopy, and density functional theory calculations. Substitution in the 3-phenyl site leads to complexes with the highest quantum yields and results in an increase in the highest occupied molecular orbital (HOMO) energy. Conversely, substitution at the 4-phenyl position lowers the lowest unoccupied orbital energy (LUMO). Some of the complexes are applied in single-layer-polymer light-emitting devices (PLEDs), which show red electrophosphorescence.

## Introduction

The discovery of electroluminescence (EL) from conjugated polymers in light-emitting devices (LEDs) has led to the rapid development of new electroactive polymers.[1] Small molecule (SMOLED) and polymer (PLED) devices have also attracted industrial interest, and some displays are already on the market.[2] The performance of SMOLEDs has been dramatically improved by using phosphorescent organometallic complexes or triplet emitters as dopants.[2,3] Efficient phosphorescence requires a significant degree of metal participation in the triplet state, as this generally reduces the singlet−triplet gap, enhances intersystem crossing, and increases emission decay rates.[4] Cyclometalated Ir(III) complexes have been widely applied as triplet emitters; they have high quantum yields and controllable emission color.[5,6] Multilayer SMOLEDs have been fabricated using green-emitting Ir(III) complexes with outstanding external quantum efficiencies (EQE) of 19%.[7] Efficient blends of phosphorescent Ir(III) complexes in conjugated polymer hosts have also been realized,[8–11] but there can be problems with film stability, phase separation, triplet−triplet annihilation at large current densities, and triplet back transfer from phosphor to conjugated polymer low-lying triplet states.[12,13] An alternative approach involves covalent attachment of the phosphor to the conjugated polymer, thereby forming an Ir(III)−polymer complex. This prevents phase separation and provides fully characterized materials with controllable separations between the polymer and the phosphorescent complex. The covalent attachment has been accomplished using either a nonconjugated spacer, often an alkyl chain, or a conjugated bond.

Attaching Ir(III) phosphors via nonconjugated linkers has been explored by several groups. Chen et al. reported the attachment of a red phosphorescent Ir(III) complex, [Ir(btp)$_2$(acac)], via an alkyl chain from the $\beta$-diketonate to a fluorene monomer.[14] Jiang and co-workers obtained EQEs of up to 4.9% using copoly(fluorene-*alt*-carbazole) with red phosphorescent Ir(III) complexes attached via alkyl linkages between the $\beta$-diketonate and a carbazole unit.[15] In a detailed study Evans et al. compared [Ir(btp)$_2$(acac)] complexes attached via the $\beta$-diketonate group either directly or through an alkyl chain to the 9-position of a 9-octylfluorene host.[16] The copolymers of the alkyl chain linked materials had efficiencies double those of the spacerless copolymers. This was attributed

* Corresponding author. E-mail: c.k.williams@imperial.ac.uk.
[†] Imperial College London.
[‡] Cambridge University.

(1) Burroughes, J. H.; Bradley, D. D. C.; Brown, A. R.; Marks, R. N.; Mackay, K.; Friend, R. H.; Burns, P. L.; Holmes, A. B. *Nature* **1990**, *347*, 539.
(2) Holder, E.; Langeveld, B. M. W.; Schubert, U. S. *Adv. Mater.* **2005**, *17*, 1109.
(3) Kohle, A.; Wilson, J. S.; Friend, R. H. *Adv. Mater.* **2002**, *14*, 701.
(4) Yersin, H. *Top. Curr. Chem.* **2004**, *241*, 1.
(5) Lamansky, S.; Djurovich, P.; Murphy, D.; Abdel-Razzaq, F.; Kwong, R.; Tsyba, I.; Bortz, M.; Mui, B.; Bau, R.; Thompson, M. E. *Inorg. Chem.* **2001**, *40*, 1704.
(6) Lamansky, S.; Djurovich, P.; Murphy, D.; Abdel-Razzaq, F.; Lee, H. E.; Adachi, C.; Burrows, P. E.; Forrest, S. R.; Thompson, M. E. *J. Am. Chem. Soc.* **2001**, *123*, 4304.
(7) Adachi, C.; Baldo, M. A.; Thompson, M. E.; Forrest, S. R. *J. Appl. Phys.* **2001**, *90*, 5048.
(8) Gong, X.; Robinson, M. R.; Ostrowski, J. C.; Moses, D.; Bazan, G. C.; Heeger, A. J. *Adv. Mater.* **2002**, *14*, 581.
(9) Gong, X.; Ostrowski, J. C.; Moses, D.; Bazan, G. C.; Heeger, A. J. *Adv. Funct. Mater.* **2003**, *13*, 439.
(10) Gong, X.; Ostrowski, J. C.; Bazan, G. C.; Moses, D.; Heeger, A. J.; Liu, M. S.; Jen, A. K. Y. *Adv. Mater.* **2003**, *15*, 45.
(11) van Dijken, A.; Bastiaansen, J.; Kiggen, N. M. M.; Langeveld, B. M. W.; Rothe, C.; Monkman, A.; Bach, I.; Stossel, P.; Brunner, K. *J. Am. Chem. Soc.* **2004**, *126*, 7718.
(12) Noh, Y. Y.; Lee, C. L.; Kim, J. J.; Yase, K. *J. Chem. Phys.* **2003**, *118*, 2853.
(13) Sudhakar, M.; Djurovich, P. I.; Hogen-Esch, T. E.; Thompson, M. E. *J. Am. Chem. Soc.* **2003**, *125*, 7796.
(14) Chen, X. W.; Liao, J. L.; Liang, Y. M.; Ahmed, M. O.; Tseng, H. E.; Chen, S. A. *J. Am. Chem. Soc.* **2003**, *125*, 636.
(15) Jiang, J. X.; Jiang, C. Y.; Yang, W.; Zhen, H. G.; Huang, F.; Cao, Y. *Macromolecules* **2005**, *38*, 4072.
(16) Evans, N. R.; Devi, L. S.; Mak, C. S. K.; Watkins, S. E.; Pascu, S. I.; Kohler, A.; Friend, R. H.; Williams, C. K.; Holmes, A. B. *J. Am. Chem. Soc.* **2006**, *128*, 6647.

10.1021/om800014e CCC: $40.75 
Publication on Web 06/06/2008

to the suppression of back transfer of triplets from the Ir(III) to the copolyfluorenes in the tethered materials.

Attaching Ir(III) phosphors directly to and in conjugation with the polymer backbone has been accomplished by Suzuki condensation polymerization between bromine-substituted Ir(III) cyclometalates and boronic ester-substituted electroactive monomers.[17] The first report from Sandee et al. involved green and red phosphorescent Ir(III) complexes conjugated to polyfluorenes; efficient energy transfer occurred only with the red emitters.[17] PLEDs showed exclusive red emission regardless of the loading of Ir(III), indicating efficient charge trapping on the Ir(III) center. Furthermore, the PLEDs fabricated with the novel materials showed higher efficiencies than blends. Several related polymer complexes have subsequently been reported using copoly(fluorene-*alt*-carbazole), copoly(fluorene-*alt*-thiophene), polycarbazole, and polyphenylene in conjugation with Ir(III) complexes.[18–26] Zhen et al. recently reported a bis(2(1-naphthalene)pyridine)iridium−polyfluorene complex that gave efficient red emission. When used in PLEDs, an external quantum efficiency of 5.3% was measured at 100 mA/cm$^2$.[23]

1-Phenylisoquinolinato Ir(III) cyclometalates were previously synthesized in high yields and showed good red color purity.[27,28] The high quantum yields, obtained using [Ir(piq)$_3$], were rationalized by the emission occurring from a predominantly $^3$MLCT (metal-to-ligand charge transfer) state, which has a radiative decay rate an order of magnitude higher than complexes that emit from a predominantly $^3$LC (ligand centered) state.[27] Despite the availability of these studies, insight into the influence of the nature and site of substitution is needed.[28–34] Here, we report a series of substituted [bis(1-phenylisoquinolinato)iridium(acetyl acetonate)] complexes (Figure 1). The complexes are substituted with bromine or fluorenyl groups at 2-, 3-, or 4-positions on the phenyl ring of the cyclometalating ligand. These regioisomers are used to probe the influence of the substituents on the photophysical properties of the complexes

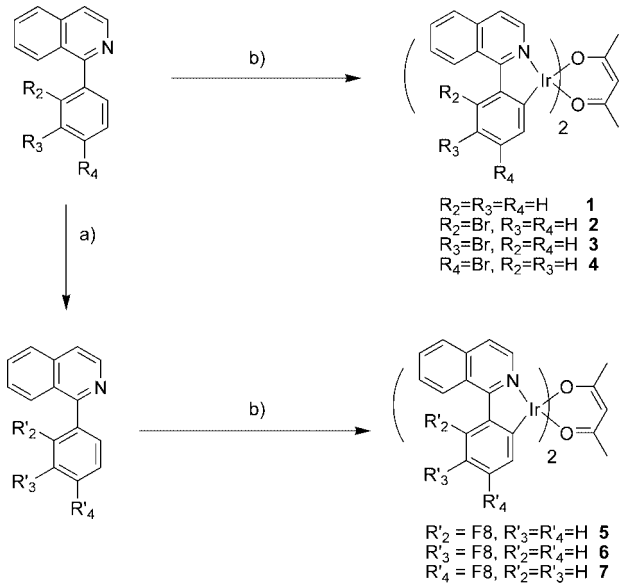


**Figure 1.** Synthesis of the well-defined iridium complexes **1**−**7**. Reagents and conditions: (a) 2-(4′,4′,5′,5′-tetramethyl-1′,3′,2′-dioxaborolan-2′-yl)-9,9-dioctylfluorene, $Pd(PPh_3)_4$ (1 mol %), $Et_4NOH$(aq), toluene, 90 °C, 18 h. 72% (R′$_2$ = fluorenyl), 80% (R′$_3$ = fluorenyl), 70% (R′$_4$ = fluorenyl). (b) (i) $IrCl_3 \cdot xH_2O$, 2-ethoxyethanol(aq), 110 °C, 18 h, (ii) acetyl acetone, 2-ethoxyethanol, $Na_2CO_3$, 110 °C, 12 h. 57% (**2**), 63% (**3**), 69% (**4**), 44% (**5**), 47% (**6**), 57% (**7**).

and as models for the polymer−iridium complexes. The new materials are characterized using optical absorption and emission spectroscopy and cyclic voltammetry. Density functional theory (DFT) using the B3LYP hybrid functional is used to model the frontier molecular orbitals in order to explain the changes in the phosphorescence. Regioisomeric polyfluorenyl−iridium complexes have also been prepared, characterized, and used as the active layer in PLEDs, where they yield red electrophosphorescence.

## Results and Discussion

**Well-Defined Ir(III) Complex Synthesis.** The bromine-substituted 1-phenylisoquinoline ligands were prepared in excellent yields by reaction and subsequent cyclization of (±)-2-amino-1-phenylethanol with the corresponding bromine-substituted benzoyl chloride (Figure S1). The fluorenyl (F8)-substituted 1-phenylisoquinoline ligands were synthesized via a Suzuki coupling condensation between the appropriate bromine 1-phenylisoquinoline regioisomer and 2-(4′,4′,5′,5′-diisopropylboronate)-9,9-dioctylfluorene. The bis(cyclometalated) Ir(III) complexes **1**−**7** were prepared in excellent yields using adaptations of literature procedures (Figure 1).[5,6]

The new ligands were reacted with $IrCl_3 \cdot xH_2O$ to yield chloro-bridged dimeric complexes, and these species were subsequently cleaved by reaction with acetyl acetone to give clean conversion to complexes **1**−**7**. All the complexes were isolated as red powders in moderate to good yield (50−90%), relative to their ligand precursors. The purity and coordination geometries were confirmed by NMR spectroscopy, elemental analysis, and mass spectrometry. The $^1$H NMR spectra confirmed the formation of $C_2$-symmetric complexes, consistent with the nitrogen atoms occupying *trans* axial coordination sites at the iridium center; such a geometry is common for heteroleptic bis(cyclometalated) Ir(III) complexes.[5,6] It was noteworthy that both **2** and **5**, which have 2-bromine and 2-fluorenyl

(17) Sandee, A. J.; Williams, C. K.; Evans, N. R.; Davies, J. E.; Boothby, C. E.; Kohler, A.; Friend, R. H.; Holmes, A. B. *J. Am. Chem. Soc.* **2004**, *126*, 7041.
(18) Zhen, H. Y.; Jiang, C. Y.; Yang, W.; Jiang, J. X.; Huang, F.; Cao, Y. *Chem.−Eur. J.* **2005**, *11*, 5007.
(19) Yang, W.; Zhen, H. Y.; Jiang, C. Y.; Su, L. J.; Jiang, J. X.; Shi, H. H.; Cao, Y. *Synth. Met.* **2005**, *153*, 189.
(20) Schulz, G. L.; Chen, X. W.; Chen, S. A.; Holdcroft, S. *Macromolecules* **2006**, *39*, 9157.
(21) Zhen, H. Y.; Luo, J.; Yang, W.; Chen, Q. L.; Ying, L.; Zou, J. H.; Wu, H. B.; Cao, Y. *J. Mater. Chem.* **2007**, *17*, 2824.
(22) Ito, T.; Suzuki, S.; Kido, J. *Polym. Adv. Tech.* **2005**, *16*, 480.
(23) Zhen, H. Y.; Luo, C.; Yang, W.; Song, W. Y.; Du, B.; Jiang, J. X.; Jiang, C. Y.; Zhang, Y.; Cao, Y. *Macromolecules* **2006**, *39*, 1693.
(24) Zhang, K.; Chen, Z.; Yang, C. L.; Gong, S. L.; Qin, J. G.; Cao, Y. *Macromol. Rapid Commun.* **2006**, *27*, 1926.
(25) Zhang, K.; Chen, Z.; Zou, Y.; Yang, C. L.; Qin, J. G.; Cao, Y. *Organometallics* **2007**, *26*, 3699.
(26) Jiang, J. X.; Yang, W.; Cao, Y. *J. Inorg. Organomet. Polym. Mater.* **2007**, *17*, 37.
(27) Tsuboyama, A.; Iwawaki, H.; Furugori, M.; Mukaide, T.; Kamatani, J.; Igawa, S.; Moriyama, T.; Miura, S.; Takiguchi, T.; Okada, S.; Hoshino, M.; Ueno, K. *J. Am. Chem. Soc.* **2003**, *125*, 12971.
(28) Su, Y. J.; Huang, H. L.; Li, C. L.; Chien, C. H.; Tao, Y. T.; Chou, P. T.; Datta, S.; Liu, R. S. *Adv. Mater.* **2003**, *15*, 884.
(29) Li, C. L.; Su, Y. J.; Tao, Y. T.; Chou, P. T.; Chien, C. H.; Cheng, C. C.; Liu, R. S. *Adv. Funct. Mater.* **2005**, *15*, 387.
(30) Yang, C. H.; Su, W. L.; Fang, K. H.; Wang, S. P.; Sun, I. W. *Organometallics* **2006**, *25*, 4514.
(31) Fang, K. H.; Wu, L. L.; Huang, Y. T.; Yang, C. H.; Sun, I. W. *Inorg. Chim. Acta* **2006**, *359*, 441.
(32) Huang, Y. T.; Chuang, T. H.; Shu, Y. L.; Kuo, Y. C.; Wu, P. L.; Yang, C. H.; Sun, I. W. *Organometallics* **2005**, *24*, 6230.
(33) Yang, C. H.; Tai, C. C.; Sun, I. W. *J. Mater. Chem.* **2004**, *14*, 947.
(34) Hu, Z. Y.; Luo, C. P.; Wang, L.; Huang, F. L.; Zhu, K. L.; Wang, Y. F.; Zhu, M. X.; Zhu, W. G.; Cao, Y. *Chem. Phys. Lett.* **2007**, *441*, 277.

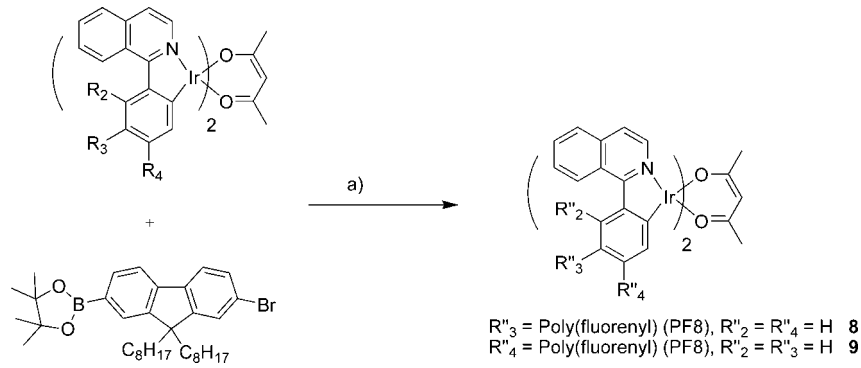


**Figure 2.** Chain extension polymerization to synthesize the [Ir(piq-PF8)$_2$(acac)] regioisomers. Reagents and conditions: (a) 18 equiv of 2-(4′,4′,5′,5′-tetramethyl-1′,3′,2′-dioxaborolan-2′-yl)-7-bromo-9,9-dioctylfluorene, 0.2 equiv of $Pd(OAc)_2$ (20 mol %), 0.4 equiv of tricyclohexylphosphine, $Et_4NOH$(aq), toluene, 110 °C; 48 h; 55% (**8**), 58% (**9**).

substituents, respectively, exhibited a significant broadening in their NMR spectra, due to the increased steric demand of that particular substitution position inducing a degree of fluxionality to the complex. Additionally, a small amount of the geometric isomer in which the cyclometalating ligands are coordinated with the N atoms *cis* to one another (5%) was isolated alongside **2**. It was identified by NMR spectroscopy due to its reduced symmetry ($C_1$ vs $C_2$) leading to an increased number of signals being observed.

**Conjugated Polymer−Ir(III) Complex Synthesis.** The successful synthesis of the series of [Ir(piq-X)$_2$(acac)] complexes enabled the preparation of the regioisomeric polyfluorene−Ir(III) complexes of the type [Ir(piq-PF8)$_2$(acac)]. The synthetic method was analogous to that reported by Sandee et al.[17] and involved a Suzuki condensation polymerization between a fluorene AB monomer 2-(4′,4′,5′,5′-tetramethyl-1′,3′,2′-dioxaborolan-2′-yl)-7-bromo-9,9-dioctylfluorene and the bromine-substituted iridium complex **3** or **4** (Figure 2).

A Suzuki polycondensation using 18 equiv of the fluorene AB monomer to 1 equiv of either **3** or **4** yielded polyfluorene−Ir(III) complexes **8** and **9** in 55% and 58% isolated yields, respectively. In both **8** and **9** the Ir(III) phosphor was bound to two polyfluorene chains; thus the metal complex acted as a chain extender. The iridium complex loadings were deduced from their $^1$H NMR spectra by integration of the methine signals on the acetyl acetonate ligand against the aromatic signals on the polyfluorene backbone. The incorporation of the iridium complex was approximately 6% by weight in both **8** and **9**, which is slightly lower than the feed loading of 8%, but confirms findings by other groups making related Ir(III)−polymer complexes.[21,23,25] The SEC data showed $M_n$ of 11 600 and 12 100 for **8** and **9**, respectively. All attempts to isolate a polymer−Ir(III) complex substituted at the 2-phenyl position, by reaction of **2** with the AB monomer, led to the isolation of a polymer without iridium incorporation, probably due to the steric hindrance of **2**.

**Absorption Spectroscopy.** The solution absorption spectra were compared for the series of small-molecule regioisomers **1**−**7** (Figure 3a, X = Br; Figure 3b, X = F8) and for the polymer−Ir(III) complexes **8** and **9** (Figure 3c, X = PF8).

The spectra are all assigned by analogy to related literature bis(cyclometalated)Ir(III) complexes.[5,6,27,28] The introduction of bromine substituents has little effect on the absorption spectra of complexes **2**−**4** compared to the unsubstituted analogue **1** (Figure 3a). The intense absorption bands between 250 and 350 nm (molar absorption coefficient, $\epsilon$ = 10 000−60 000 $M^{-1}$ $cm^{-1}$) are attributed to $^1\pi-\pi^*$ transitions between 1-phenylisoquinolinato-centered states. The weaker absorption bands ($\epsilon$ = 1000−6000 $M^{-1}$ $cm^{-1}$) in the range 350−440 nm are assigned to the spin-allowed metal-to-ligand charge transfer transitions, $^1$MLCT, and those at 450−500 nm to the spin-forbidden metal-to-ligand charge transfer transitions, $^3$MLCT, which gain intensity through the strong spin−orbit coupling.[5,6,28,35,36] Substitution of the 1-phenylisoquinolinato ligands with fluorenyl groups, on the other hand, significantly alters the absorption spectra for **5**−**7** (Figure 3b). As for **1**−**4**, the intense absorption bands between 250 and 300 nm are attributed to $^1\pi-\pi^*$ transitions of 1-phenylisoquinolinato-centered states. The absorption bands between 320 and 400 nm are attributed to $^1\pi-\pi^*$ transitions of the fluorenyl substituents. Complexes **5** and **7** each display red-shifted fluorenyl absorption peaks. For **5** this peak is also of reduced intensity. The weaker MLCT absorption bands in the range 450−600 nm are also red-shifted compared to **1**. These red-shifts indicate extended conjugation, i.e., orbital overlap between the fluorenyl substituents and the iridium complex. Figure 3c shows the solution absorption spectra of the polyfluorene−Ir(III) complexes **8** and **9**. They display absorption maxima at approximately 380 nm, which are attributed to $\pi-\pi^*$ transitions of the polyfluorene. The maxima are red-shifted compared with the fluorenyl absorptions of **5**−**7** due to the extended conjugation along the polyfluorene backbone. Lower intensity absorptions are present at 430−440 nm, which are attributed to $\pi-\pi^*$ transitions of the polyfluorene in its $\beta$-phase. Their relative intensity is consistent with previously reported spectra.[37]

**Emission Spectroscopy.** The optically excited phosphorescence spectra of **1**−**7** were measured in $CH_2Cl_2$ solutions at 298 K, using an excitation wavelength of 350 nm (Figure 4).

The unsubstituted complex **1** has an emission maxima at 623 nm, close to that reported previously for **1** (622 nm).[28] Complexes **2**, **3**, and **5**−**7** all display red-shifted emissions, while complex **4** displays a blue-shift. The influence of the site of substitution on the shift in the emission differs between the bromine- and fluorenyl-substituted complexes. For the bromine substituents, the $\lambda_{max}$ varies in the order **2** > **3** > **1** > **4**, and for the fluorenyl substituents, the order is **7** > **6** > **5** ≫ **1**. It is also worth noting that complexes **2** and **5** have identical emission maxima.

The optically induced emission spectra of the polymer complexes **8** and **9** differ according to the conditions of the measurements (Figure 5).

(35) Colombo, M. G.; Hauser, A.; Gudel, H. U. *Inorg. Chem.* **1993**, *32*, 3088.
(36) Schmid, B.; Garces, F. O.; Watts, R. J. *Inorg. Chem.* **1994**, *33*, 9.
(37) Hayer, A.; Khan, A. L. T.; Friend, R. H.; Kohler, A. *Phys. Rev. B* **2005**, *71*, 241302.

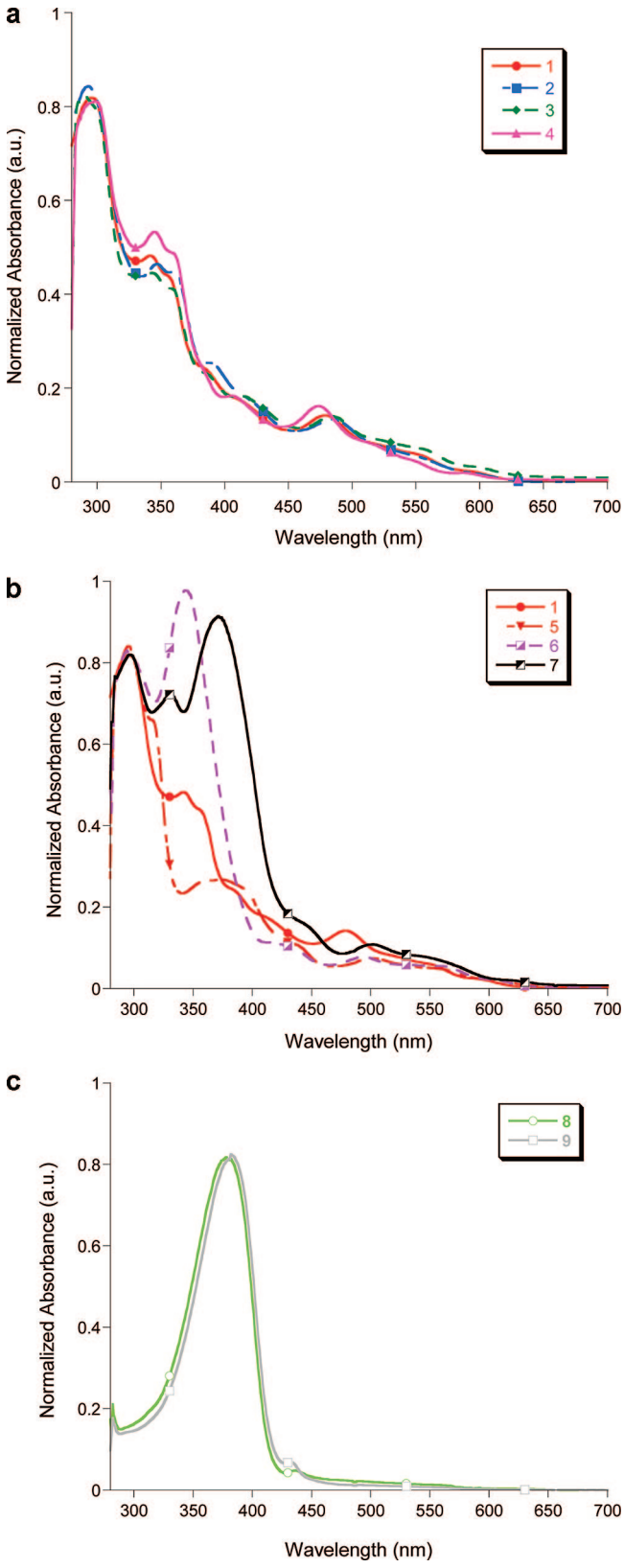


**Figure 3.** UV−vis absorption spectra of **1**−**4** (a), **1** and **5**−**7** (b), and **8** and **9** (c). The spectra were determined in 0.0001 M $CH_2Cl_2$ solutions at 298 K.

In solution, both **8** and **9** emit almost exclusively from their polyfluorene backbones, showing an intense blue fluorenyl fluorescence signal at 416 nm with only a low-intensity red phosphorescence signal. This is due to the lack of energy transfer from the polyfluorene chain to the central phosphor.[13] In the

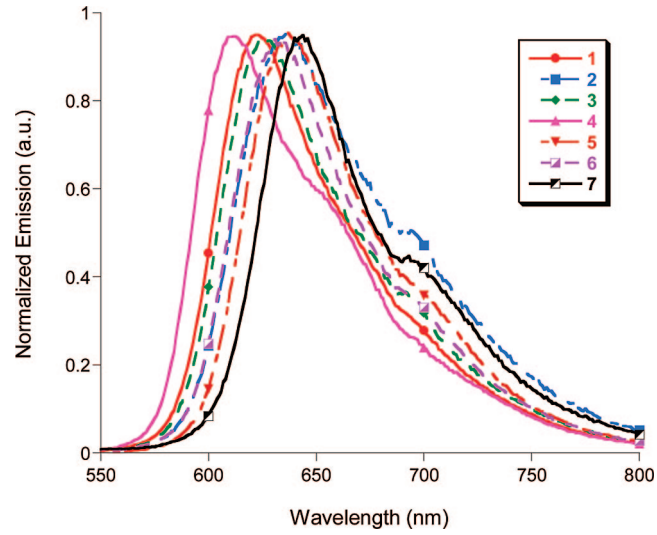


**Figure 4.** Solution phosphorescence spectra of compounds **1**−**7**. The spectra were determined in degassed $CH_2Cl_2$ solutions at 298 K. All excitation energies were 350 nm.

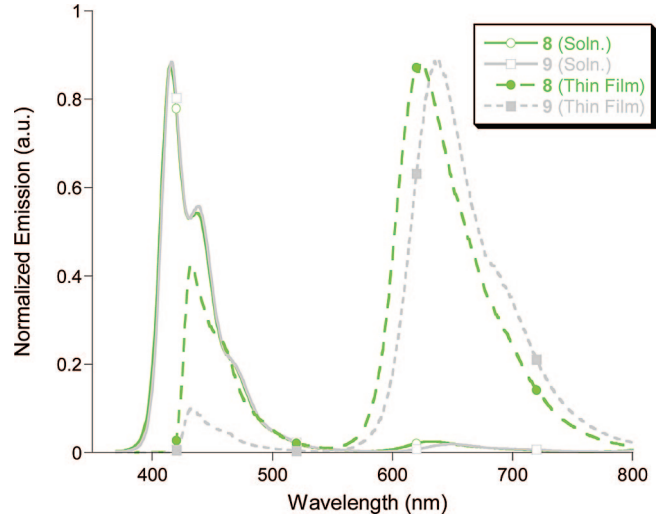


**Figure 5.** Thin film and solution phosphorescence spectra of compounds **8** and **9**. The solution spectra were determined in degassed $CH_2Cl_2$ solutions at 298 K. Thin films were spin coated from $CH_2Cl_2$ solutions of a 10 mg/mL dilution. All excitation energies were 350 nm.

solid state (thin films, spin coated from $CH_2Cl_2$ solutions), **8** and **9** display predominantly red phosphorescence, at 625 and 639 nm, respectively, and originating from their Ir(III) phosphors, with only low-intensity polyfluorene emission. This is due to the close proximity of molecules, which allows greater energy transfer from the polyfluorene chain to the central iridium phosphor.[13,16] The residual thin film emissions originating from the polyfluorene chain are also red-shifted by approximately 15 nm compared to the solution spectra, due to aggregation effects.[38,39] The phosphorescence spectra of **8** and **9** correspond well with those of their small-molecule analogues **6** and **7**, indicating that the well-defined Ir(III) complexes are viable models for the polymer−Ir(III) complexes.

**Quantum Yields.** The solution phosphorescence quantum yields, Φ, of **2**−**7** were measured in degassed methylene

(38) Grell, M.; Bradley, D. D. C.; Long, X.; Chamberlain, T.; Inbasekaran, M.; Woo, E. P.; Soliman, M. *Acta Polym.* **1998**, *49*, 439.
(39) Blondin, P.; Bouchard, J.; Beaupre, S.; Belletete, M.; Durocher, G.; Leclerc, M. *Macromolecules* **2000**, *33*, 5874.

**Table 1. Solution Absorbance and Emission Wavelengths and Quantum Yields of Complexes 1−9 (absorption and emission spectra were determined in $CH_2Cl_2$ solutions at room temperature)**

| compound | absorbance wavelength (molar absorption coefficient, $\epsilon/M^{-1}cm^{-1}$)$\lambda_{max}$/nm | phosphorescence emission wavelength $\lambda_{max}$/nm | quantum yields, $\Phi$[a] |
|---|---|---|---|
| **1** | 234 (32 054) | 623 | 0.20 |
| | 291 (20 570) | | |
| | 351 (10 474) | | |
| | 477 (2524) | | |
| **2** | 248 (45 318) | 637 | 0.07 |
| | 296 (30 816) | | |
| | 351 (16 919) | | |
| | 395 (9063) | | |
| | 490 (4834) | | |
| **3** | 235 (59 528) | 626 | 0.14 |
| | 274 (37 487) | | |
| | 351 (16 249) | | |
| | 412 (6275) | | |
| | 482 (2896) | | |
| **4** | 236 (48 521) | 612 | 0.10 |
| | 295 (33 518) | | |
| | 348 (18 675) | | |
| | 405 (6704) | | |
| | 472 (4310) | | |
| **5** | 233 (47 144) | 637 | 0.03 |
| | 289 (33 447) | | |
| | 376 (8601) | | |
| | 477 (1752) | | |
| **6** | 294 (23 423) | 634 | 0.15 |
| | 336 (24 187) | | |
| | 426 (2164) | | |
| | 481 (1273) | | |
| **7** | 235 (36 132) | 644 | 0.06 |
| | 298 (26 083) | | |
| | 332 (22 021) | | |
| | 371 (2586) | | |
| | 495 (2138) | | |
| **8** | 382 | 416 (soln) | n/a |
| | 441 | 625 (thin film) | 0.22 |
| **9** | 385 | 416 (soln) | n/a |
| | 436 | | 0.10 |
| | | 639 (thin film) | |

[a] $\Phi$ was determined in degassed $CH_2Cl_2$ solutions using **1** as the standard. Thin films were spin coated from $CH_2Cl_2$ solutions of a 10 mg/mL dilution. Thin film $\Phi$'s were determined using an integrating sphere. All excitation energies were 350 nm.

chloride solutions using **1** as the standard (Table 1). Complexes **2** and **5** have low quantum yields and display significant peak broadening in their $^1$H NMR spectra, which are attributed to fluxional processes. It is believed that this is due to steric interactions between the substituent at the 2-phenyl position and the isoquinoline ring, which results in an increase in nonradiative relaxation pathways. Complexes **3**, **4**, **6**, and **7** all show moderate quantum yields ($\Phi = 0.06-0.15$). The quantum yields for the thin films of the polymer complexes **8** and **9** ($\Phi = 0.10-0.22$) are comparable to those of the fluorenyl-substituted model compounds. Substitution in the 3-phenyl position leads to the highest quantum yields for all the substituted complexes. The origin of this phenomenon is currently being explored.

**Energy Levels.** In order to understand the variation in optical properties of the regioisomers, it was important to establish the properties of the frontier molecular orbitals. The orbital energies were determined by cyclic voltammatry and absorption spectroscopy. Density functional theory (DFT) calculations, using the hybrid functional B3LYP, were used to model the linear combination of atomic orbitals (LCAO) and the pattern of the molecular orbitals. A measure for the HOMO energy, $E_{HOMO}$, is the ionization potential; here the ionization potential was calculated from the half-wave oxidation potential ($E_{1/2}$) as determined by cyclic voltammetry, conducted in methylene chloride solution (Table 2, Figure 6).[40] Complexes **1**−**7** all showed cyclic voltammograms with a single, reversible one-electron oxidation peak. No reduction processes were detected within the solvent cathodic limit. Polymer complexes **8** and **9** displayed irreversible one-electron oxidations, but again no reduction waves were detected. Therefore, the optical energy gap of the complexes was estimated from the absorption onset in the absorption spectra, and this was used to obtain the LUMO energy, $E_{LUMO}$ (Table 2, Figure 6).[41] Both the nature of the substituents and their positions on the phenyl ring exert a significant influence over the orbitals' energies and therefore over the optical properties.

**Table 2. Molecular Orbital Energies (eV) and the Phenyl Isoquinoline C−C Bond Torsion Angles (deg) for Complexes 1−9**

| compound | $\Delta E$[a]/ eV | $E_{HOMO}$[b]/eV | $E_{LUMO}$[c]/eV | torsion angle[d]/ deg |
|---|---|---|---|---|
| **1** | 1.99 | −5.11 | −3.12 | 16 |
| **2** | 1.96 | −5.33 | −3.37 | 32 |
| **3** | 1.97 | −5.27 | −3.3 | 16 |
| **4** | 2.02 | −5.38 | −3.36 | 16 |
| **5** | 1.95 | −5.10 | −3.15 | 29 |
| **6** | 1.95 | −5.06 | −3.11 | 18 |
| **7** | 1.93 | −5.19 | −3.26 | 17 |
| **8** | 2.75 | −5.70 | −2.95 | n/a |
| **9** | 2.77 | −5.72 | −2.95 | n/a |

[a] Determined from the absorption onset wavelength in the UV−vis spectrum, in $CH_2Cl_2$, room temperature.[41] [b] Determined from cyclic voltammetry, in $CH_2Cl_2$ solution.[40] [c] $E_{LUMO} = E_{HOMO} + \Delta E$. [d] Determined from the optimized geometries obtained by DFT calculations.

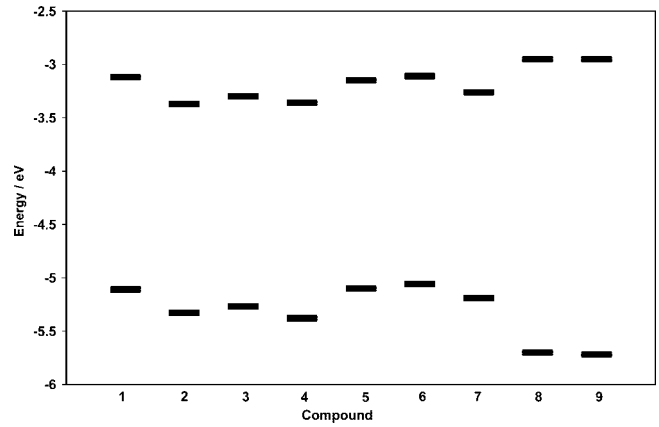


**Figure 6.** HOMO and LUMO energies for compounds **1**−**9**. HOMO energies calculated from the $E_{1/2}$ obtained by cyclic voltammetry (in $CH_2Cl_2$ solutions)[40] and LUMO energies obtained from the optical energy gap,[41] estimated from the absorption onset energy obtained by UV−vis spectroscopy (in $CH_2Cl_2$ solution).

B3LYP calculations were performed on **1**−**7**. The frontier molecular orbital contour plots (Figure 7) were generated from geometry optimizations on the singlet ground state. Such an approach has previously been successful for modeling other phosphorescent Ir(III) complexes.[31,42] For the entire series, the HOMOs are predominantly localized on the two phenyl rings but also have a significant contribution from the d-atomic orbitals of Ir(III). The lowest unoccupied molecular orbitals (LUMOs) are mostly localized on the isoquinoline rings; however, there are LCAO coefficients at the 2- and 4-phenyl positions and a node at the 3-phenyl site. The calculated trends

(40) D'Andrade, B. W.; Datta, S.; Forrest, S. R.; Djurovich, P.; Polikarpov, E.; Thompson, M. E. *Org. Electron.* **2005**, *6*, 11.
(41) Burrows, P. E.; Shen, Z.; Bulovic, V.; McCarty, D. M.; Forrest, S. R.; Cronin, J. A.; Thompson, M. E. *J. App. Phys.* **1996**, *79*, 7991.
(42) Hay, P. J. *J. Phys. Chem. A* **2002**, *106*, 1634.

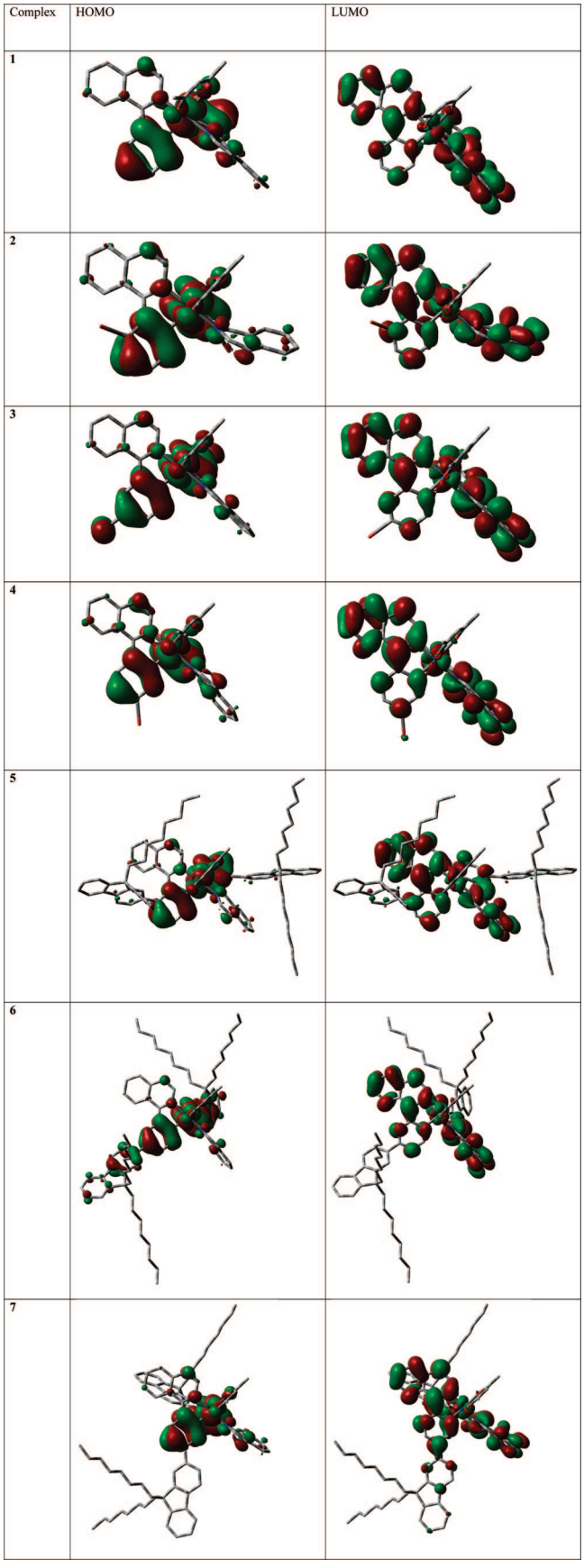


**Figure 7.** Contour plots of the HOMOs and LUMOs for complexes **1**−**7**. The color and size of the lobes reflect the sign and amplitude of the linear combination of atomic orbital (LCAO) coefficients, respectively.

in the orbital energies (Figure S2) were in excellent agreement with those observed experimentally (Figure 6). Indeed, the calculated $E_{HOMO}$ values showed exactly the same variations as those in Figure 6, while the trend for the $E_{LUMO}$ was in good agreement except for **3** and **6**, which showed values that were lower than observed.

The bromine-substituted regioisomers **2** and **3** have significantly lower $E_{HOMO}$ and $E_{LUMO}$ than the unsubstituted complex **1**. This is due to the inductive, electron-withdrawing effect of the bromine atom stabilizing the frontier orbitals, resulting in a net lowering of $E_{HOMO}$ and $E_{LUMO}$. For complex **4**, the Br substituent exerts predominantly an inductive effect, which affects the HOMO to a greater extent than the LUMO and results in a net separation of its frontier orbitals. This is supported by the DFT calculations, which show LCAO coefficients for both the HOMO and LUMO at the 4-phenyl position. The HOMO and LUMO levels of **3** are lowered less than **4**. For **3**, the Br substituent can exert both an inductive and mesomeric effect. The significant contribution of the Br 4p atomic orbitals to the HOMO can clearly be seen in **3** (Figure 7). The mesomeric effect leads to a destabilization of the HOMO. A similar destabilization was observed by Avilov et al., who carried out DFT calculations on fluorinated phenyl pyridine iridium cyclometallates.[43] Furthermore, for **3** the presence of a node in the LUMO at the 3-position means the LUMO is less affected by the inductive effect of the bromine than **2** and **4**. The consequence is a smaller energy gap for **3**; this is verified by a bathochromic shift in its emission.

$E_{HOMO}$ and $E_{LUMO}$ for the fluorenyl-substituted complexes **5**−**7** are similar to those of the substituted derivative **1**. The DFT calculations show molecular orbitals with significant coefficients on the fluorenyl rings. Fluorenyl substituents in conjugation with the phenyl ring result in a stabilization of the LUMO energy level and a destabilization of the HOMO energy. Complex **6** has a raised HOMO energy, but its LUMO is unchanged from **1**. DFT calculations show that the LUMO of **6** has the same distribution as **1** (i.e., predominantly localized on the isoquinoline ring but with a node at the 3-phenyl position). The fluorenyl substituent in **6** therefore cannot strongly influence the LUMO energy. However, DFT shows that its HOMO is significantly delocalized onto the fluorenyl substituent. This results in its higher HOMO energy and the bathochromic shift in the emission. Conversely, **7** has a HOMO that is isoelectronic with that of **1**, but its LUMO energy is lower due to significant delocalization onto the fluorenyl substituents. Experimentally this is observed in the bathochromic shift in its emission. In general, the stabilizing effect on the LUMO by fluorenyl substituents has a greater magnitude than the destabilizing of the HOMO; therefore a greater bathochromic shift occurs in the emission of **7** relative to **6**. Complexes **2** and **5** have identical emission maxima despite the significant difference in the energy levels of their frontier orbitals.

The torsion angles of the C−C bond that joins the phenyl and isoquinoline rings were measured from the optimized geometries obtained from the DFT calculation (Table 2). Complexes **1**, **3**, **4**, **6**, and **7** all have torsion angles of 16−18°, demonstrating that substitutions at the 3- and 4-phenyl positions do not impose any additional steric demands. Complexes **2** and **5** have significantly increased torsion angles (32°) due to the hindrance between substituents at the 2-phenyl position and the phenyl and isoquinoline rings. It is believed that this increased torsion leads to a reduction in the HOMO−LUMO energy gap and produces the observed red-shift. Similar bathochromic shifts have been observed by Fang et al.[31] As mentioned previously,

(43) Avilov, I.; Minoofar, P.; Cornil, J.; De Cola, L. *J. Am. Chem. Soc.* **2007**, *129*, 8247.

it is also likely that the observed broadening of the NMR spectra and the reduced quantum yields for complexes **2** and **5** is a consequence of their large torsion angles.

Cyclic voltammetry indicates that complexes **8** and **9** have the same HOMO and LUMO energies as polyfluorene. Oxidation and reduction processes originating from the Ir(III) in these complexes are not observed due to their low loading levels. The measured orbitals are higher and lower in energy than the LUMO and HOMO of **1**−**7**, which implies that charge trapping will be a significant process in electrophosphorescence. The relative order of the emission energies of **8** and **9** mirrors those observed with the small molecule complexes; that is, the substitution at the 4-phenyl position results in a greater bathochromic shift in the emission wavelength (smaller energy gap) than the 3-phenyl position. Therefore, **9** emits at longer wavelength than **8**, as was observed for the small molecules with **7** emitting at longer wavelength than **6**. In the thin films, compound **8** displays significantly more fluorenyl singlet emission, but its quantum yield for phosphorescence is significantly greater than compound **9**. We propose that the lower LUMO energy of compound **9** (*vide supra*) facilitates energy transfer from the polyfluorene to the phosphor, leading to a reduction in the polyfluorene singlet emission. However, compound **9** shows a lower quantum yield, in an analogous manner to compound **7**.

**Electrophosphorescence.** The LEDs used for electrophosphorescence characterization consisted of a basic planar structure, as shown in the inset in Figure 8a.

Figure 8a also shows the electrophosphorescence spectra obtained for the homologous series of compounds **5**−**7**, while Figure 8b shows the spectra for compounds **8** and **9**. In both cases, the observed electrophosphorescence spectra closely matched the corresponding optically induced phosphorescent emission in the solid state. Thus, complexes **8** and **9** showed red electrophosphorescence with emission maxima at 636 and 648 nm, respectively. Further work is currently in progress in order to optimize the functional design of these prototypical LEDs, so that the maximum attainable luminances and quantum efficiencies can be quantitatively determined.

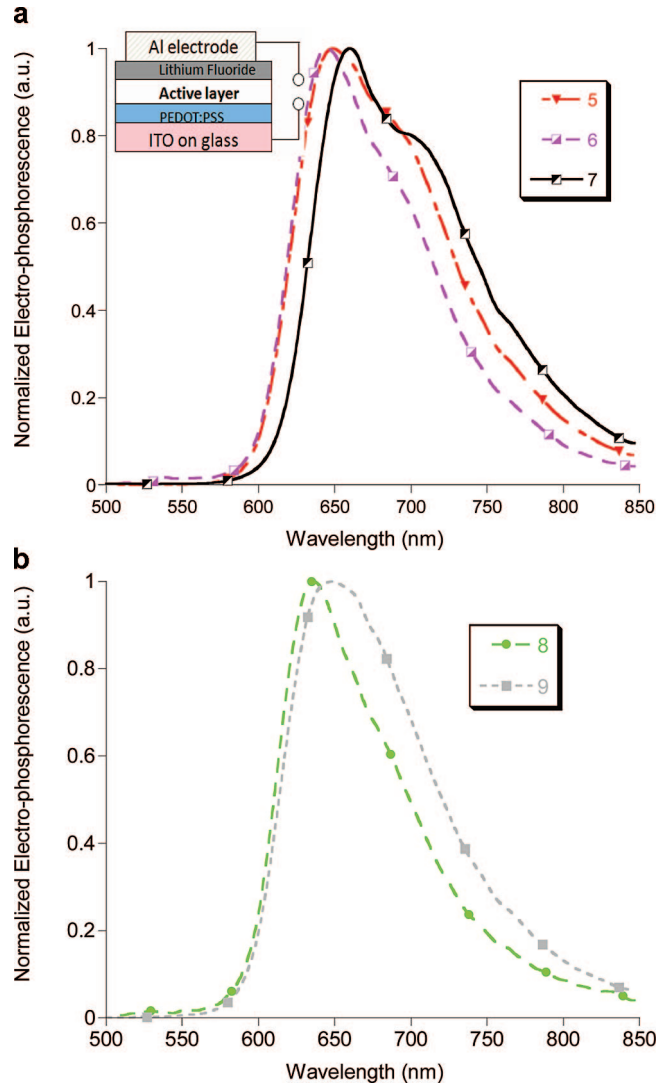


**Figure 8.** Electrophosphorescence spectra for compounds **5**−**7**, together with an inset showing the schematic structure of the planar LEDs (a). Electrophosphorescence spectra for compounds **8** and **9** (b), with the Commission Internationale de l'Eclairage (CIE) coordinates of ($x = 0.652$, $y = 0.323$) and ($x = 0.676$, $y = 0.325$), respectively.

## Conclusions

A series of regioisomeric [Ir(piq-X)$_2$(acac)] complexes have been synthesized and their photophysical properties related to their chemical structures. The nature and site of the substituents exert a significant influence over the emission from the iridium complexes. The site of substitution was systematically varied around the phenyl ring of the 1-phenylisoquinolinato cyclometalating ligand. Substituents at the 3-position exerted a greater influence over the HOMO; electrochemistry and optical methods show its energy is raised by substitution at this site. DFT calculations showed a mesomeric effect, which results in 3-phenyl substituents influencing the electron density in the C−Ir bond. The 3-subsitution site exerted a minimal influence on the LUMO energy. DFT calculations showed a node at this site. The 4-phenyl substitution site has a greater influence on the LUMO, reducing its energy with both a bromine and a fluorenyl substituent. The DFT calculations showed a LCAO coefficient at the 4-phenyl position; thus the bromine substituent reduces the LUMO energy by an inductive effect and the fluorenyl substituent by a mesomeric effect. The 2-phenyl substitution position shows severe steric hindrance, by both spectroscopic and theoretical methods. This results in a similarly reduced HOMO−LUMO energy gap for different substituents, which appears to be more dependent on the torsion angle than its chemical nature. The emission quantum yields also depend on the site of substitution, with much better yields being observed for substituents in the 3-phenyl site than the 2-phenyl or 4-phenyl positions. The synthesis of polymeric−Ir(III) complexes of the type [Ir(piq-PF8)$_2$(acac)] was achieved in good yield by Suzuki polycondensation between an AB monomer and a bromine-substituted Ir(III) regioisomer. The materials have efficient energy transfer from the polyfluorene to the phosphor, and they show red phosphorescence in the solid state. The emission energies of the regioisomeric polymer complexes mirror those observed with the small molecule complexes; that is, the substitution at the 4-phenyl position results in a greater bathochromic shift in the emission wavelength (smaller energy gap) than the 3-phenyl position. The electrophosphorescence spectra of compounds **5**−**9** show the same trends as the optically induced emission spectra.

## Experimental Section

**Materials.** All reactions were conducted under a nitrogen atmosphere, using either standard anaerobic techniques or in a

nitrogen-filled glovebox. All solvents and reagents were obtained from commercial sources (Aldrich and Merck). Toluene was dried by distillation from sodium, and chloroform-$d_3$ was dried by distillation from calcium hydride. $IrCl_3 \cdot xH_2O$ was loaned by Johnson Matthey Plc. 2-(4′,4′,5′,5′-Tetramethyl-1′,3′,2′-dioxaborolan-2′-yl)-9,9-dioctylfluorene,[44] 2-(4′,4′,5′,5′-tetramethyl-1′,3′,2′-dioxaborolan-2′-yl)-7-bromo-9,9-dioctylfluorene,[17] and [Ir(III) bis(1-(phenyl)isoquinolinato-*N,C*′)(acetylacetonate)] (**1**)[28] were prepared according to the literature methods. The preparations of 2-bromo-*N*-(2-hydroxy-2-phenylethyl)benzamide, 1-(2-bromophenyl)isoquinoline, 1-(3-bromophenyl)isoquinoline, and 1-(4-bromophenyl-)isoquinoline are described in the Supporting Information.

**Measurements.** $^1H$ and $^{13}C\{^1H\}$ NMR spectra were performed on a Bruker Av-400 instrument. Elemental analyses were determined by Mr. Stephen Boyer at London Metropolitan University, North Campus, Holloway Road, London, N7. SEC data were collected using a Polymer Laboratories PL GPC-50 instrument with THF as the eluent, at a flow rate of 1 mL $min^{-1}$. Two Polymer Laboratories mixed D columns were used in series, and the $M_n$ values were calibrated against narrow $M_n$ polystyrene standards (Easy-Cal standards A and B). Chemical ionization (CI) and fast atom bombardment (FAB) mass spectra were recorded on a Micromass Autospec Premier instrument.

**Absorption and Emission Spectroscopy.** UV−visible spectra were recorded, at room temperature, on a Thermo Unicam UV500 spectrometer, in methylene chloride solutions at concentrations of 0.0001 M. Thin films of polymers **8** and **9** were spin coated from methylene chloride solutions of 10 mg/mL on a Laurell spin coater at 2000 rpm for 30 s.

Optically induced phosphorescence spectra were collected using a CaryEclipse fluorescence spectrophotometer. Solution phosphorescence measurements were done on methylene chloride solutions. The excitation wavelength was 350 nm, and the spectra were recorded at room temperature. Solution quantum yields were determined in degassed methylene chloride solutions with maximum absorbance of 0.2 using the Parker−Rees method.[45] Compound **1** was used as the standard ($\Phi_P = 0.2$ in methylene chloride).[28] Thin film quantum yields were determined using an integrating sphere with an excitation wavelength of 350 nm using the method developed by de Mello et al.[46] All spectra were corrected.

**Theoretical Methods.** Density functional theory (DFT) using the B3LYP hybrid functional was applied for all calculations. Geometry optimizations were performed without any constraint. All calculations were performed using the 6-31G basis set for the ligands and the LANL2DZ basis set for Ir(III),[42] as implemented by Gaussian 03.[47]

**Cyclic Voltammetry.** Cyclic voltammety measurements were recorded in degassed, anhydrous methylene chloride, with 1 M tetrabutylammonium hexafluorophosphate as the supporting electrolyte (at a scan rate of 100 mV/s). The working electrode was platinum, with a platinum wire counter electrode and a saturated Ag/AgCl pseudoreference electrode. Ferrocene was used as an internal standard. No reduction wave was observed from 0 to −2 V. Complexes **1**−**7** showed reversible oxidations, whereas complexes **8** and **9** displayed nonreversible oxidations. The oxidation potentials were converted into ionization potentials by relating the electrochemical energy scale to the vacuum energy scale, according to the method described by D'Andrade et al.[40] The LUMO energy level ($E_{LUMO}$) was calculated by adding the optical energy gap ($\Delta E$) (calculated from the absorption edge) to the HOMO energy level.[41]

**Electrophosphorescence.** A 60 nm layer of poly(3,4-ethylenedioxythiophene)/poly(styrene sulfonate) (PEDOT:PSS) was spin-coated onto ITO (indium−tin oxide)-coated glass, as a hole-injecting, semitransparent electrode. A thin film (∼80 nm thickness) of the compound under study was then spin-coated, from chlorobenzene solution, onto the PEDOT:PSS layer. The electron-injecting electrode was deposited by thermally evaporating approximately 1 nm of LiF, followed by 80 nm of aluminum. The prepared LED devices were encapsulated and tested under vacuum conditions at room temperature. The device testing was performed using a high-sensitivity parameter analyzer and a spectrally calibrated photodiode. Electrophosphorescence spectra were recorded using a fiber-coupled CCD spectrometer (ORIEL), with a spectral resolution of around 1 nm. All the devices were operated at similar driving biases of a few volts, and spectra were generally observed to be independent of driving bias.

**Ligand Syntheses. 1-(2-(9′,9′-Dioctylfluoren-2′-yl)phenyl)isoquinoline.** 1-(2-Bromophenyl)isoquinoline (0.25 g, 1.77 mmol), 2-(4′,4′,5′,5′-tetramethyl-1′,3′,2′-dioxaborolan-2′-yl)-9,9-dioctylfluorene (0.41 g, 1.77 mmol), and $Pd(PPh_3)_4$ (10 mg, 0.01 mmol) were suspended in toluene (10 mL) and $Et_4NOH$ (2 mL of a 20% solution in water), and the reaction mixture was stirred at 90 °C for 18 h. The solution was extracted with $CH_2Cl_2$ (50 mL), washed with water (3 × 50 mL), dried ($MgSO_4$), and concentrated *in vacuo*. Column chromatography (silica gel, petroleum ether/EtOAc, 6:1) afforded the product as a colorless oil (0.75 g, 72%).

Anal. Calcd for $C_{44}H_{51}N$: C 88.99, H 8.66, N 2.36. Found: C 88.97, H 8.63, N 2.30. $^1H$ NMR (400 MHz, $CDCl_3$, ppm): $\delta$ 8.61 (d, $J = 5.8$ Hz, 1H, Ar*H*), 7.63 (m, 9H, Ar*H*), 7.44 (m, 2H, Ar*H*), 7.23 (m, 4H, Ar*H*), 6.96 (s, 1H, Ar*H*), 1.64 (m, 6H, C$H_3$), 1.2 (m, 14H, C$H_2$), 0.90 (m, 14H, C$H_2$). $^{13}C\{^1H\}$ NMR (125 MHz, $CDCl_3$ ppm): $\delta$ 161.6, 150.7, 150.0, 142.0, 141.9, 140.6, 139.9, 139.4, 138.2, 135.9, 130.7, 130.1, 129.7, 128.7, 127.6, 127.5, 126.7, 126.5, 123.7, 122.7, 119.9, 119.4, 119.2, 54.6, 40.3, 40.0, 31.9, 31.8, 30.0, 29.3, 29.2, 23.4, 23.3, 22.6, 14.1. *m/z* (CI): 594 $[M + H]^+$.

**1-(3-(9′,9′-Dioctylfluoren-2′-yl)phenyl)isoquinoline.** Prepared according to the same procedure used for 1-(2-(9′,9′-dioctylfluoren-2′-yl)phenyl)isoquinoline. The title compound was a colorless oil (0.79 g, 80%).

Anal. Calcd for $C_{44}H_{51}N$: C 88.99, H 8.66, N 2.36. Found: C 88.99, H 8.65, N 2.31. $^1H$ NMR (400 MHz, $CDCl_3$, ppm): $\delta$ 8.64 (d, $J = 5.7$ Hz, 1H, Ar*H*), 8.17 (d, $J = 8.5$ Hz, 1H, Ar*H*), 7.74 (m, 12H, Ar*H*), 7.33 (m, 3H, Ar*H*), 2.04 (m, 6H, C$H_3$), 1.03 (m, 28H, C$H_2$). $^{13}C\{^1H\}$ NMR (125 MHz, $CDCl_3$ ppm): $\delta$ 161.8, 150.4, 159.6, 142.1, 141.9, 140.6, 134.0, 139.4, 138.2, 135.6, 130.7, 130.1, 129.7, 128.7, 127.6, 127.5, 126.7, 126.5, 123.7, 122.7, 119.8, 119.4, 119.2, 54.6, 40.3, 40.0, 31.8, 30.0, 29.4, 29.1, 23.4, 23.1, 22.8, 14.0. *m/z* (CI): 594 $[M + H]^+$.

**1-(4-(9′,9′-Dioctylfluoren-2′-yl)phenyl)isoquinoline.** This compound was prepared according to the same procedure used for 1-(2-(9′,9′-dioctylfluoren-2′-yl)phenyl)isoquinoline. The title compound was isolated as a white crystalline solid (0.68 g, 70%).

Anal. Calcd for $C_{44}H_{51}N$: C 88.99, H 8.66, N 2.36. Found: C 89.01, H 8.67, N 2.31. $^1H$ NMR (400 MHz, $CDCl_3$, ppm): $\delta$ 8.67 (d, $J = 5.7$ Hz, 1H, Ar*H*), 8.24 (d, $J = 8.5$ Hz, 1H, Ar*H*), 7.95 (d, $J = 8.1$ Hz, 1H, Ar*H*), 7.75 (m, 10H, Ar*H*), 7.60 (t, $J = 7.7$ Hz,

(44) Ranger, M.; Leclere, M. *Can. J. Chem.* **1998**, *76*, 1571.
(45) Parker, C. A.; Rees, W. T. *Analyst* **1960**, *85*, 587.
(46) deMello, J. C.; Wittmann, H. F.; Friend, R. H. *Adv. Mater.* **1997**, *9*, 230.
(47) Frisch, M. J.; Trucks, G. W.; Schlegel, H. B.; Scuseria, G. E.; Robb, M. A.; Cheeseman, J. R.; Montgomery, Jr., J. A.; Vreven, T.; Kudin, K. N.; Burant, J. C.; Millam, J. M.; Iyengar, S. S.; Tomasi, J.; Barone, V.; Mennucci, B.; Cossi, M.; Scalmani, G.; Rega, N.; Petersson, G. A.; Nakatsuji, H.; Hada, M.; Ehara, M.; Toyota, K.; Fukuda, R.; Hasegawa, J.; Ishida, M.; Nakajima, T.; Honda, Y.; Kitao, O.; Nakai, H.; Klene, M.; Li, X.; Knox, J. E.; Hratchian, H. P.; Cross, J. B.; Bakken, V.; Adamo, C.; Jaramillo, J.; Gomperts, R.;Stratmann, R. E.; Yazyev, O.; Austin, A. J.; Cammi, R.; Pomelli, C.; Ochterski, J. W.; Ayala, P. Y.; Morokuma, K.; Voth, G. A.; Salvador, P.; Dannenberg, J. J.; Zakrzewski, V. G.; Dapprich, S.; Daniels, A. D.; Strain, M. C.; Farkas, O.; Malick, D. K.; Rabuck, A. D.; Raghavachari, K.; Foresman, J. B.; Ortiz, J. V.; Cui, Q.; Baboul, A. G.; Clifford, S.; Cioslowski, J.; Stefanov, B. B.; Liu, G.; Liashenko, A.; Piskorz, P.; Komaromi, I.; Martin, R. L.; Fox, D. J.; Keith, T.; Al-Laham, M. A.; Peng, C. Y.; Nanayakkara, A.; Challacombe, M.; Gill, P. M. W.; Johnson, B.; Chen, W.; Wong, M. W.; Gonzalez, C.; Pople, J. A. Gaussian 03; Gaussian, Inc.: Wallingford, CT, 2004.

1H, Ar*H*), 7.38 (m, 3H, Ar*H*), 2.06 (m, 4H, C$H_2$), 1.09 (m, 20H, C$H_2$), 0.83 (m, 6H, C$H_3$), 0.74 (m, 4H, C$H_2$). $^{13}C\{^1H\}$ NMR (125 MHz, $CDCl_3$ ppm): $\delta$ 151.5, 151.0, 142.3, 141.9, 140.7, 139.4, 136.9, 130.4, 130.0, 127.6, 127.2, 127.1, 126.8, 126.0, 122.9, 121.5, 120.0, 119.9, 119.8, 61.0, 55.2, 40.4, 31.7, 30.0, 29.2, 23.8, 22.6, 14.0. *m/z* (CI): 594 $[M + H]^+$.

**Ir(III) Complex Syntheses. [Ir(III)bis(1-(2′-bromophenyl)isoquinolinato-*N,C*)(acetylacetonate)], 2.** A mixture of $IrCl_3 \cdot xH_2O$ (0.08 g, 0.23 mmol) and 1-(2-(bromophenyl)isoquinoline (0.30 g, 0.51 mmol) in 2-ethoxyethanol (7.5 mL) and water (2.25 mL) was heated to 110 °C for 18 h. After the mixture cooled to room temperature, the precipitate was filtered and washed with EtOH/$H_2O$ (95:5, 30 mL). The precipitate was then dissolved in $CH_2Cl_2$ (50 mL), dried ($MgSO_4$), and concentrated *in vacuo* to yield [bis(Ir(III)di-$\mu$-chlorotetrakis(1-(2-(bromophenyl)isoquinolinato-*N,C*)] as a dark red solid (0.11 g, 60%). [Bis(Ir(III)di-$\mu$-chlorotetrakis(1-(2-(bromophenyl)isoquinolinato-*N,C*)] (0.11 g, 0.115 mmol) was dissolved in 2-ethoxyethanol (10 mL) in the presence of acetyl acetone (0.09 mL, 0.58 mmol) and $Na_2CO_3$ (0.12 g, 1.15 mmol). The resulting suspension was stirred at 110 °C for 12 h. The reaction mixture was cooled to room temperature, and water (10 mL) was added. The resulting red precipitate was filtered, washed with $H_2O$ (30 mL), and then dissolved in $CH_2Cl_2$ (30 mL), dried ($MgSO_4$), filtered, and concentrated *in vacuo*. Purification by flash column chromatography (silica gel, $CH_2Cl_2$/hexane, 5:1) afforded [*trans*-Ir(III)bis(1-(2′-bromophenyl)isoquinolinato-*N,C*)(acetyl acetonate)] (0.11 g, 57%) and [*cis*-Ir(III)bis(1-(2′-bromophenyl)isoquinolinato-*N,C*)(acetyl acetonate)] (0.04 g, 20%) as red solids.

**[*trans*-Ir(III)bis(1-(2′-bromophenyl)isoquinolinato-*N,C*)(acetylacetonate)].** Anal. Calcd for $C_{35}H_{25}Br_2IrN_2O_2$: C 49.02, H 2.94, N 3.27. Found: C 48.99, H 2.95, N 3.25. $^1H$ NMR (400 MHz, $CDCl_3$, ppm): $\delta$ 8.42 (d, $J = 8.3$ Hz, 2H, Ar*H*), 8.32 (d, $J = 6.3$ Hz, 2H, Ar*H*), 7.90 (d, $J = 8.1$ Hz, 2H, Ar*H*), 7.71 (t, $J = 7.7$ Hz, 2H, Ar*H*), 7.60 (t, $J = 7.6$ Hz, 4H, Ar*H*), 7.11 (d, $J = 7.1$ Hz, 2H, Ar*H*), 6.47 (br, 2H, Ar*H*), 5.245 (br s, 1H, OC($CH_3$)C*H*), 1.773 (br s, 6H, OC(C$H_3$)CH). $^{13}C\{^1H\}$ NMR (125 MHz, $CDCL_3$ ppm): $\delta$ 140.3, 140.0, 137.2, 131.3, 131.0, 130.7, 130.2, 129.7, 129.1, 127.7, 127.2, 127.0, 126.8, 125.9, 120.6, 119.9, 100.6, 28.6. *m/z* (FAB): 857 $[M + H]^+$.

**Ir(III)bis(1-(3′-bromophenyl)isoquinolinato-*N,C*)(acetylacetonate)], 3.** This compound was synthesized according to the method used to prepare compound **2**. It was isolated as a red solid (0.17 g, 63%).

Anal. Calcd for $C_{35}H_{25}Br_2IrN_2O_2$: C 49.02, H 2.94, N 3.27. Found: C 48.95, H 2.94, N 3.23. $^1H$ NMR (400 MHz, $CDCl_3$, ppm): $\delta$ 8.91 (m, 2H, Ar*H*), 8.41(d, $J = 6.4$ Hz, 2H, Ar*H*), 8.30 (d, $J = 1.9$ Hz, 2H, Ar*H*), 7.96 (m, 2H, Ar*H*), 7.76 (m, 4H, Ar*H*), 7.53 (d, $J = 6.3$ Hz, 2H, Ar*H*), 6.77 (d, $J = 8.1$ Hz, 2H, Ar*H*), 6.23 (d, $J = 8.2$ Hz, 2H, Ar*H*), 5.21 (s, 1H, OC($CH_3$)C*H*), 1.76 (s, 6H, OC(C$H_3$)CH). $^{13}C\{^1H\}$ NMR (125 MHz, $CDCl_3$ ppm): $\delta$ 149.50, 148.58, 140.34, 137.16, 135.11, 132.01, 131.68, 130.99, 128.31, 127.45, 126.35, 120.70, 114.14. *m/z* (FAB): 857 $[M + H]^+$.

**[Ir(III)bis(1-(4′-bromophenyl)isoquinolinato-*N,C*)(acetylacetonate)], 4.** This complex was synthesized according to the method used to prepare compound **2**. It was isolated as a red solid (0.18 g, 69%).

Anal. Calcd for $C_{35}H_{25}Br_2IrN_2O_2$: C 49.02, H 2.94, N 3.27. Found C 48.97, H 2.93, N 3.19. $^1H$ NMR (400 MHz, $CDCl_3$, ppm): $\delta$ 9.03 (d, $J = 4.6$ Hz, 2H, Ar*H*), 8.51 (d, $J = 6.3$ Hz, 2H, Ar*H*), 8.26 (d, $J = 8.3$ Hz, 2H, Ar*H*), 7.98 (d, $J = 4.6$ Hz, 2H, Ar*H*), 7.77 (m, 4H, Ar*H*), 7.55 (d, $J = 6.0$ Hz, 2H, Ar*H*), 7.11 (d, $J = 8.0$ Hz, 2H, Ar*H*), 6.56 (s, 2H, Ar*H*), 5.26 (s, 1H, OC($CH_3$)C*H*), 1.81 (s, 6H, OC(C$H_3$)CH). $^{13}C\{^1H\}$ NMR (125 MHz, $CDCl_3$ ppm): $\delta$ 184.8, 169.0, 168.8, 151.9, 146.3, 140.6, 137.1, 131.5, 131.3, 130.7, 129.9, 128.7, 127.8, 127.4, 126.7, 126.4, 120.0, 119.5. *m/z* (FAB): 857 $[M + H]^+$.

**[Ir(III)bis(1-(2-(9′,9′-dioctylfluoren-2′-yl)phenyl)isoquinolinato-*N,C*)(acetylacetonate)], 5.** This complex was synthesized according to the method used to prepare compound **2**. It was isolated as a red solid (0.36 g, 44%).

Anal. Calcd for $C_{93}H_{107}IrN_2O_2$: C 75.62, H 7.30, N 1.90. Found: C 75.63, H 7.35, N 1.92. $^1H$ NMR (400 MHz, $CDCl_3$, ppm): $\delta$ 8.48 (d, $J = 6.3$ Hz, 2H, Ar*H*), 8.07 (br, m, 2H, Ar*H*), 7.62 (br m, 6H, Ar*H*), 7.46 (br m, 4H, Ar*H*), 7.24 (m, 10H, Ar*H*), 7.01 (br m, 6H, Ar*H*), 6.75 (br m, 2H, Ar*H*), 5.39 (br s, 1H, OC($CH_3$)C*H*), 1.92 (br m, 12H, C$H_2$/C$H_3$), 1.28 (br m, 48H, OC(C$H_3$)CH, C$H_3$, C$H_2$), 0.42 (br m, 8H, C$H_2$). $^{13}C\{^1H\}$ NMR (125 MHz, $CDCl_3$, ppm): $\delta$ 185.1, 185.1, 171.6, 150.8, 143.1, 143.1, 140.7, 140.3, 138.9, 136.1, 131.7, 129.9, 129.7, 128.8, 128.7, 126.5, 125.6, 125.1, 124.8, 122.9, 120.0, 119.5, 107.9, 100.6, 54.6, 54.5, 39.9, 31.9, 31.7, 30.3, 30.0, 29.7, 29.5, 29.2, 28.7, 23.5, 22.7, 22.6, 14.1. *m/z* (FAB): 1477 $[M + H]^+$.

**[Ir(III)bis(1-(3-(9′,9′-dioctylfluoren-2′-yl)phenyl)isoquinolinato-*N, C*)(acetylacetonate)], 6.** This compound was synthesized according to the method used to prepare compound **2**. It was isolated as a red solid (0.27 g, 47%).

Anal. Calcd for $C_{93}H_{107}IrN_2O_2$: C 75.62, H 7.30, N 1.90. Found: C 75.6, H 7.18, N 1.91. $^1H$ NMR (400 MHz, $CDCl_3$, ppm): $\delta$ 9.18 (m, 2H, Ar*H*), 8.59 (d, $J = 8.6$ Hz, 2H, Ar*H*), 8.57 (s, 2H, Ar*H*), 8.01 (m, 2H, Ar*H*), 7.75 (m, 8H, Ar*H*), 7.59 (m, 4H, Ar*H*), 7.53 (s, 2H, Ar*H*), 7.32 (m, 6H, Ar*H*), 7.08 (d, $J = 7.9$ Hz, 2H, Ar*H*), 6.61 (d, $J = 6.6$ Hz, 2H, Ar*H*), 5.31 (s, 1H, OC($CH_3$)C*H*), 1.97 (m, 8H, C$H_2$), 1.86 (s, 6H, OC(C$H_3$)CH), 1.11 (m, 40H, C$H_2$), 0.81 (m, 12H, C$H_3$), 0.70 (m, 8H, C$H_2$). $^{13}C\{^1H\}$ NMR (125 MHz, $CDCl_3$, ppm): $\delta$ 184.9, 169.2, 151.3, 151.2, 150.9, 147.2, 141.4, 141.0, 140.6, 139.3, 137.3, 134.1, 133.9, 130.7, 128.6, 128.3, 127.7, 127.4, 126.8, 126.7, 126.5, 125.3, 122.8, 121.2, 120.0, 119.8, 119.5, 100.6, 54.9, 40.4, 31.7, 30.1, 29.2, 28.8, 23.8, 22.6, 14.0. *m/z* (FAB): 1477 $[M + H]^+$.

**[Ir(III)bis(1-(4-(9′,9′-dioctyl-fluoren-2′-yl)phenyl)isoquinolinato-*N, C*)(acetylacetonate)], 7.** This compound was synthesized according to the method used to prepare compound **2**. It was isolated as a red solid (0.21 g, 57%).

Anal. Calcd for $C_{93}H_{107}IrN_2O_2$: C 75.62, H 7.30, N 1.90. Found: C 75.58, H 7.15, N 1.88. $^1H$ NMR (400 MHz, $CDCl_3$, ppm): $\delta$ 9.09 (m, 2H, Ar*H*), 8.59 (d, $J = 6.2$ Hz, 2H, Ar*H*), 8.33 (d, $J = 8.5$ Hz, 2H, Ar*H*), 7.99 (m, 2H, Ar*H*), 7.81 (m, 4H, Ar*H*), 7.61(d, $J = 7.1$ Hz, 2H, Ar*H*), 7.55 (d, $J = 6.3$ Hz, 2H, Ar*H*), 7.51 (d, $J = 7.9$ Hz, 2H, Ar*H*), 7.29 (m, 16H, Ar*H*), 7.12 (d, $J = 1.2$ Hz, 2H, Ar*H*), 6.76 (d, $J = 1.9$ Hz, 2H, Ar*H*), 5.32 (s, 1H, OC($CH_3$)C*H*), 1.86 (s, 6H, OC(C$H_3$)CH), 1.80 (m, 4H, C$H_2$), 1.61 (m, 4H, C$H_2$), 0.7−1.7 (m, 52H, C$H_2$/C$H_3$), 0.46 (m, 8H, C$H_2$). $^{13}C\{^1H\}$ NMR (125 MHz, $CDCl_3$, ppm): $\delta$ 184.8, 169.1, 152.1, 150.8, 150.6, 145.8, 140.8, 140.1, 139.4, 137.1, 131.1, 130.6, 129.9, 127.7, 127.4, 126.7, 126.5, 126.4, 125.6, 122.6, 121.1, 120.9, 119.5, 119.3, 100.6, 99.9, 54.7, 40.5, 40.3, 31.8, 30.1, 30.0, 29.3, 29.2, 28.8, 23.6, 22.6, 14.1. *m/z* (FAB): 1477 $[M + H]^+$.

**Polyfluorene−Ir(III) Complex Synthesis. [Ir(III)bis(1-(3′-(ω-bromo-oligo[9″,9″-dioctylfluoren-2″,7″-diyl])phenyl)isoquinolinato-*N,C*)(acetylacetonate)], 8.** A solution of 2-(4′,4′,5′,5′-tetramethyl-1′,3′,2′-dioxaborolan-2′-yl)-7-bromo-9,9-dioctylfluorene (1.04 g, 1.74 mmol, 18 equiv), Ir(III)bis(1-(3′-bromophenyl)isoquinolinato-*N,C*)(acetylacetonate) (83 mg, 0.097 mmol, 1 equiv), $Pd(OAc)_2$ (5 mg, 0.022 mmol), and tricyclohexylphosphine (12 mg, 0.044 mmol) in toluene (75 mL) was heated to 90 °C. To this, $Et_4NOH$ (7.50 mL of a 20% solution in water) was added and the solution stirred at 110 °C for 48 h. The reaction mixture was cooled to room temperature and subsequently poured into a large excess of MeOH, which resulted in the precipitation of the polymer. The precipitate was filtered, washed with water

(40 mL), MeOH (40 mL), and acetone (30 mL), and filtered through Celite using toluene as the eluent. The resulting solution was concentrated (to 20 mL), and $Na_2CO_3$ (0.20 g), acetyl acetone (2.00 mL), and 2-ethoxyethanol (10 mL) were added. The reaction mixture was stirred for 2 h at 110 °C and subsequently cooled to room temperature. The solution was again poured into an excess of MeOH and the precipitate filtered, washed with $H_2O$ (40 mL) and MeOH (40 mL), and dried *in vacuo*. The pure product was isolated as a red powder (0.42 g, 55%).

Anal. Calcd for $C_{557}H_{745}Br_2IrN_2O_2$: C 85.19, H 9.56, N 0.36. Found: C 83.42, H 9.68, N 0.26. $^1$H NMR (400 MHz, $CDCl_3$, ppm): $\delta$ 9.14, 8.54, 7.90−7.60 (m, 6H, Ar*H*), 7.04, 6.56, 5.27 (s, OC($CH_3$)C*H*), 2.30−2.00 (m, 4H, C$H_2$), 1.83 (s, OC(C$H_3$)CH), 1.30−1.00 (m, 20H, C$H_2$), 0.90−0.70 (m, 10H, C$H_3$C$H_2$). $^{13}$C{$^1$H} NMR (125 MHz, $CDCl_3$, ppm): $\delta$ 151.8, 140.5, 140.0, 126.2, 121.5, 119.9, 55.3, 40.5, 40.4, 31.8, 30.1, 29.2, 23.9, 22.6, 14.1. GPC (PS): $M_n$ = 11 555, $M_w$ = 21 439, PDI = 1.85.

**[Ir(III)bis(1-(4′-(ω-bromo-oligo[9″,9″-dioctylfluoren-2″,7″-diyl])phenyl)isoquinolinato-*N*,*C*)(acetylacetonate)], 9.** This complex was synthesized according to the same procedure used to produce [Ir(III)bis(1-(3′-(ω-bromo-oligo[9″,9″-dioctylfluoren-2″,7″-diyl])phenyl)isoquinolinato-*N*,*C*)(acetylacetonate)] and isolated as a red powder (0.44 g, 58%).

Anal. Calcd for $C_{557}H_{745}Br_2IrN_2O_2$: C 85.19, H 9.56, N 0.36. Found: C 83.42, H 9.36, N 0.23. $^1$H NMR (400 MHz, $CDCl_3$, ppm): $\delta$ 9.10 (Ar*H*), 8.59 (Ar*H*), 8.32 (Ar*H*), 7.90−7.60 (m, 6H, Ar*H*), 7.15 (Ar*H*), 6.78 (Ar*H*), 5.32 (s, OC($CH_3$)C*H*), 2.30−2.00 (m, 4H, C$H_2$), 1.86 (s, OC(C$H_3$)CH), 1.30−1.00 (m, 20H, C$H_2$), 0.90−0.70 (m, 10H, $CH_3CH_2$). $^{13}$C{$^1$H} NMR (125 MHz, $CDCl_3$, ppm): $\delta$ 151.8, 140.5, 140.0, 126.2, 121.5, 119.9, 55.4, 40.4, 31.8, 30.1, 29.2, 23.9, 22.6, 14.1. GPC (PS): $M_n$ = 12 112, $M_w$ = 21 266, PDI = 1.7.

**Acknowledgment.** The EPSRC is acknowledged for funding the research (EP/C548132/1). Johnson Matthey Plc. is thanked for the donation of $IrCl_3 \cdot xH_2O$. Prof. Henry Rzepa and Dr. Sarah Wilsey at the EPSRC National Service for Computational Chemistry Software (NSCCS) are thanked for their help with the DFT calculations. Dr. Paul Wilde is thanked for the assistance with cyclic voltammetry measurements. Dr. Siva Krishnadasan is thanked for assistance with the thin film quantum yield determination.

**Supporting Information Available:** Scheme (Figure S1) and experimental protocols for the preparation of the bromine-substituted ligands. Figure S2 shows the variation in calculated orbital energies. This material is available free of charge via the Internet at http://pubs.acs.org.

OM800014E